Am J Physiol Cell Physiol 331: C1680–C1687, 2026.
First published October 9, 2026; doi:10.1152/ajpcell.00336.2026

american physiological society

AMERICAN JOURNAL OF PHYSIOLOGY
CELL PHYSIOLOGY

RESEARCH ARTICLE

Women's Health Research and Novel Perspectives on Sex as an Investigative Variable

Diminished nutrient supply stimulates endothelial metabolic rate turnover: impact of cellular sex on glucose and glutamine metabolism

Mario Lorenz,[1,2,3] Janine Wiebach,[4,5] Angelika Vietzke,[1,2] Cornelia Bartsch,[1,2] Verena Stangl,[1,2,3] Karl Stangl,[1,2] Wolfgang Henrich,[1,6] Jennifer A. Kirwan,[4,5,7] and Raphaela Fritsche-Guenther[4,5]

[1]*Charité–Universitätsmedizin Berlin, Corporate Member of Freie Universität Berlin and Humboldt-Universität zu Berlin, Berlin, Germany;* [2]*Deutsches Herzzentrum der Charité, Klinik für Kardiologie, Angiologie und Intensivmedizin, CCM, Berlin, Germany;* [3]*DZHK (German Centre for Cardiovascular Research), Partner site Berlin, Berlin, Germany;* [4]*BIH Metabolomics, Berlin Institute of Health at Charité–Universitätsmedizin Berlin, Berlin, Germany;* [5]*Max Delbrück Center for Molecular Medicine in the Helmholtz Association, Berlin, Germany;* [6]*Department of Obstetrics, Charité–Universitätsmedizin Berlin, Berlin, Germany; and* [7]*University of Veterinary Medicine Vienna, Vienna, Austria*

Abstract

Endothelial cells must be able to maintain metabolic activity during angiogenesis. At impaired energy levels, they have to form new blood vessels to supply the surrounding tissue with oxygen and nutrients. This requires modifications of intracellular metabolism to provide the necessary energy for migration and proliferation. Studies on metabolic adaptations of endothelial cells to diminished energy supply are sparse, and investigation of potential sex differences is lacking. We therefore performed a metabolic flux analysis with ^{13}C-glucose or ^{13}C-glutamine labeling at different time points with female and male human umbilical vein endothelial cells from dizygotic twin pairs. Labeling was performed under basal conditions and after serum starvation at early and late time points for each labeling. Overall, a much faster label incorporation was found in serum-starved cells. Central carbon metabolites showed a significantly higher label incorporation at both early and late time points for ^{13}C-glucose and ^{13}C-glutamine after serum starvation, independent of the sex of the cells. However, a nonsignificant but consistent sex-specific pattern was observed. After labeling with ^{13}C-glucose, a higher label incorporation was seen in male cells after serum starvation. In contrast, labeling with ^{13}C-glutamine resulted in a faster label incorporation in female cells, both at basal conditions and after serum starvation. The observed sex differences were coherent throughout the analyzed metabolites. Although not significant and rather small, they could point to subtle sex differences in glucose vs. glutamine metabolism in cellular metabolic adaptations to reduced energy supply.

NEW & NOTEWORTHY Endothelial cells show small but consistent sex differences in metabolic flux. Although male cells had a faster metabolic incorporation under serum starvation after ^{13}C-glucose labeling, female cells showed a faster labeling incorporation after ^{13}C-glutamine. In light of the essential role of glutamine for overall cellular function, the faster label incorporation of glutamine in female cells could contribute to the described superior capacity of female cells to cope with unfavorable environmental conditions.

endothelial metabolism; flux analysis; glucose and glutamine; serum starvation; sex differences

INTRODUCTION

Metabolic adaptations are crucial to cope with a diminished supply of nutrients and energy in organisms and cells. Fasting in humans triggers a metabolic switch from using glucose to burning fat for energy supply (1). On the cellular level, timely and adequate changes in intracellular metabolic pathways are vital to cope with (patho)physiological challenges (2). Endothelial cells of the vascular wall are subjected to constant blood flow, concurrent with quantitative and qualitative alterations in nutrient and electrolyte compositions. Despite low oxygen and nutrient levels, their role is essential in forming new vasculature (3, 4). The angiogenic process is associated with elevated energy expenditure, mainly via the glycolytic pathway (5–7). Angiogenesis of blood vessels is under close metabolic guidance (8). Previously, we observed a faster metabolic label incorporation in endothelial cells after serum starvation compared with the basal state, indicating an acceleration of intracellular metabolite turnover (9). However, the sex of the cells was not taken into account. Sex and gender differences are increasingly recognized in the human metabolome and in metabolic disorders (10, 11). Sex-specific differences in blood metabolites were found in newborns immediately after birth, indicating that they exist before the hormonal changes

Correspondence: R. Fritsche (raphaela.fritsche@bih-charite.de).
Submitted 5 June 2026 / Revised 2 September 2026 / Accepted 22 September 2026

0363-6143/26 Copyright © 2026 The Authors. Licensed under Creative Commons Attribution CC-BY 4.0.
Published by the American Physiological Society.

during adolescence (12). However, metabolic studies addressing potential sex differences at the cellular level are still sparse. In a previous work, we have shown that female human umbilical vein endothelial cells (HUVECs) had higher ATP levels compared with male cells after serum starvation (13). This could suggest that female HUVECs may have a better stress tolerance and a more favorable energetic balance under conditions of nutrient deprivation.

Here we used human umbilical vein endothelial cells (HUVECs) from opposite sex twin pairs to study potential metabolic sex differences after serum starvation. These twin cells were exposed in utero to the same maternal environment, making them an excellent model to study potential sex disparities. Using ^{13}C-glucose or ^{13}C-glutamine, we traced the incorporation of the labeled carbons into central carbon metabolites and analyzed the effects of serum starvation as a model for reduced cellular energy supply. The dynamic metabolic activity of HUVECs was measured using a pulsed stable isotope-resolved metabolic analysis (pSIRM) with labeled ^{13}C-carbons in a time-wise manner under basal conditions and after serum starvation.

MATERIALS AND METHODS

Isolation and Cultivation of HUVECs

Endothelial cells were isolated from umbilical cord veins by digestion with collagenase type II (0.5 mg/mL, Biochrom KG, Berlin, Germany) at 37°C for 20 min. Detached cells were released by flushing the veins twice with Hank's balanced salt solution (HBSS). The mixture was centrifuged at 1,200 *g* for 5 min, and the cell pellets were resuspended in medium M199. After isolation, the cells were grown in M199 (Thermo Fisher Scientific, Waltham, MA) supplemented with 20% fetal calf serum (FCS), 12 μg/mL ECGS (endothelial cell growth supplement, PromoCell, Heidelberg, Germany), 5 U/mL heparin, 2 mM L-glutamine, 5 μg/mL ascorbic acid, 5 μg/mL glutathione, 100 U/ml penicillin, 100 μg/mL streptomycin, and 50 ng/mL amphotericin B (Biochrom, Merck, Berlin, Germany). For the determination of the cellular sex mRNA levels of SRY (sex determining region Y that is expressed from the Y-chromosome only) and XIST (X-inactive-specific transcript, expression is restricted to female cells) were determined by TaqMan Gene Expression Assays from Applied Biosystems (SRY Hs00976796, XIST Hs01079824, β-actin (Hs01060665; Thermo Fisher Scientific, Waltham, MA) served as the reference gene. Isolation of male and female HUVECs from dizygotic twin pairs of the opposite sex was approved by the Charité University Hospital Ethics Committee (EA2/017/13) and conformed to local university guidelines and the principles outlined in the Declaration of Helsinki. The mothers provided their written informed consent.

Labeling and Extraction

First, 10^6 cells were seeded in 10 cm^2 culture dishes and grown until confluence. Then, 24 h before the experiments, cells were washed twice with phosphate-buffered saline (PBS, Thermo Fisher Scientific, Waltham, MA) and incubated in M199 with either 20% or 0.5% FCS. At the beginning of the experiment (time zero), cells were changed to the label medium (M199 without glucose and glutamine, Caisson Laboratories, MDP01-10X1L, Smithfield, UT). The label medium was supplemented with 5.5 mM glucose for labeling with ^{13}C-glutamine, 2.68 mM glutamine for labeling with ^{13}C-glucose, or 5.5 mM glucose and 2.68 mM glutamine for no labeling. Labeling was performed with 5.5 mM ^{13}C-glucose (U13C6 D-glucose, Cambridge Isotope Laboratories, Tewksbury, MA) or with 2.68 mM ^{13}C-glutamine (^{13}C L-glutamine, Cambridge Isotope Laboratories, Tewksbury, MA). Cells were incubated for the indicated time points with the corresponding labeled media. At the end of the experiments, cells were rapidly washed (20 s) with wash buffer (140 mM NaCl and 5 mM HEPES, pH 7.4, room temperature) containing either ^{13}C-glucose/^{12}C-glutamine, ^{12}C-glucose/^{13}C-glutamine, or ^{12}C-glucose/^{12}C-glutamine (zero time point) at the same concentration as in the original media. Cells were lysed with 5 mL ice-cold 50% methanol (MeOH, Th. Geyer, Berlin, Germany) solution. Immediately after the MeOH solution was added to the culture plate, lysates were scraped into the methanol solution, and the methanolic lysates were collected and stored at −20°C. Subsequently, 4 mL of chloroform ($CHCl_3$, VWR International, Radnor, PA), 1.5 mL of MeOH, and 1.5 mL of water (H_2O, VWR International, Radnor, PA) were added to the methanolic cell extracts, shaken for 60 min at 4°C, and centrifuged at 4,149 *g* for 10 min to separate the phases. The polar phase (6 mL) was collected and dried at 30°C at a speed of 1,550 *g* at 0.1 mbar using a rotational vacuum concentrator (RVC 2-33 CDplus, Christ, Osterode am Harz, Germany). Samples were pooled after extraction and used as a quality control sample to measure the technical variability of the instrument. They were prepared alongside the samples in the same way. After drying, samples were split by adding 600 μL of 20% MeOH to the dried extracts and shaking for 60 min at 4°C, followed by centrifugation at maximum speed (18,213 *g*) for 10 min. Two 280 μL aliquots per sample were then dried under vacuum; one was analyzed and the other kept as a backup.

GC-MS Metabolomics Measurement of Key Central Carbon Pathway Metabolites

All polar cell extracts were stored dry at −80°C until analysis. Extracts were removed from the freezer and dried in a rotational vacuum concentrator for 60 min before further processing to ensure there was no residual water, which may influence the derivatization efficiency. Dried extracts were dissolved in 20 μL of a methoxyamine hydrochloride (Sigma-Aldrich, St. Louis, MO) solution (40 mg/mL in pyridine, Sigma-Aldrich, St. Louis, MO) and incubated for 90 min at 30°C with constant shaking, followed by the addition of 80 μL of N-methyl-N-(trimethylsilyl)trifluoroacetamide (MSTFA, Machery-Nagel, Düren, Germany) and incubation at 37°C for 60 min. The extracts were centrifuged for 10 min at 10,000 *g*, and aliquots of 30 μL were transferred into glass vials for GC-MS measurement. An identification mixture for compound identification was prepared and derivatized in the same way, and an alkane mixture for reliable retention index calculation was included (14). A metabolite analysis was performed on a Pegasus BT GCxGC TOFMS system (LECO Corporation, St. Joseph, MN) complemented by an autosampler (Gerstel MPS DualHead with CAS4 injector, Mühlheim an der Ruhr, Germany). The samples were injected in split mode (split 1:5, injection volume: 1 μL) in a temperature-controlled injector with a baffled glass liner (Gerstel, Mühlheim an der Ruhr,

Germany). The following temperature program was applied during sample injection: for 2 min, the column was allowed to equilibrate at 70°C; then the temperature was increased by 5°C/min until 120°C; then it was increased by 7°C/min up to 200°C; then it was increased by 12°C/min up to a maximum temperature of 320°C, which was then held for 7.5 min. Gas chromatographic separation was performed on an Agilent 8890 (Agilent Technologies, Santa Clara, CA) equipped with a VF-5ms column (Agilent Technologies, Santa Clara, CA) with a 30 m length, a 250 μm inner diameter, and a 0.25 μm film thickness. Helium was used as the carrier gas, with a flow rate of 1.2 mL/min. The spectra were recorded in a mass range of 60 to 600 *m*/*z* at 10 spectra/s. The GC-MS chromatograms were processed with ChromaTOF software (LECO Corporation, St. Joseph, MN), including a baseline assessment, peak picking, and a computation of the area. Label incorporation was determined according to the mass pairs after the application of ^{13}C-glucose or ^{13}C-glutamine (Supplemental Table S1) (15). Targeted metabolites from the central carbon metabolism (α-ketoglutaric acid, citric acid, fumaric acid, glycerol, lactic acid, malic acid, pyruvic acid, and succinic acid) were selected for further data analysis, and the number of biological replicates per metabolite and condition is provided (Supplemental Tables S2 and S3).

Statistics

In total, data from 16 twin pairs were processed and manually edited. For each metabolite, the corresponding identification mixture was used to calculate the sum of the specific mass range, including the associated label pair. For all the samples, the same height for the specific mass range was extracted manually and summed up to calculate the proportion for each mass (in %). The following formula was used to calculate the naturally occurring label incorporation, subtract it from the real label incorporation, and calculate the label incorporation per sample:

$$\mathrm{R} = \mathrm{X}\,(\text{proportion of mass } {}^{13}\mathrm{C} \text{ identification mixture})/ \mathrm{Y}\,(\text{proportion of mass } {}^{12}\mathrm{C} \text{ identification mixture}) \times \mathrm{Z}\,(\text{proportion of mass } {}^{12}\mathrm{C} \text{ sample})$$

$$\mathbf{S} = W\,(\text{proportion of mass } {}^{13}\mathrm{C} \text{ sample}) - R$$

$$\text{Label incorporation (LI) (\%)} = \mathrm{S}/(\mathrm{S} + \mathrm{Z}) \times 100.$$

Label incorporation values below zero were set to zero. If no peak was available, label incorporation was set to NA. All statistical analyses were performed using R (R version 4.5.1; R Foundation for Statistical Computing, Vienna, Austria)

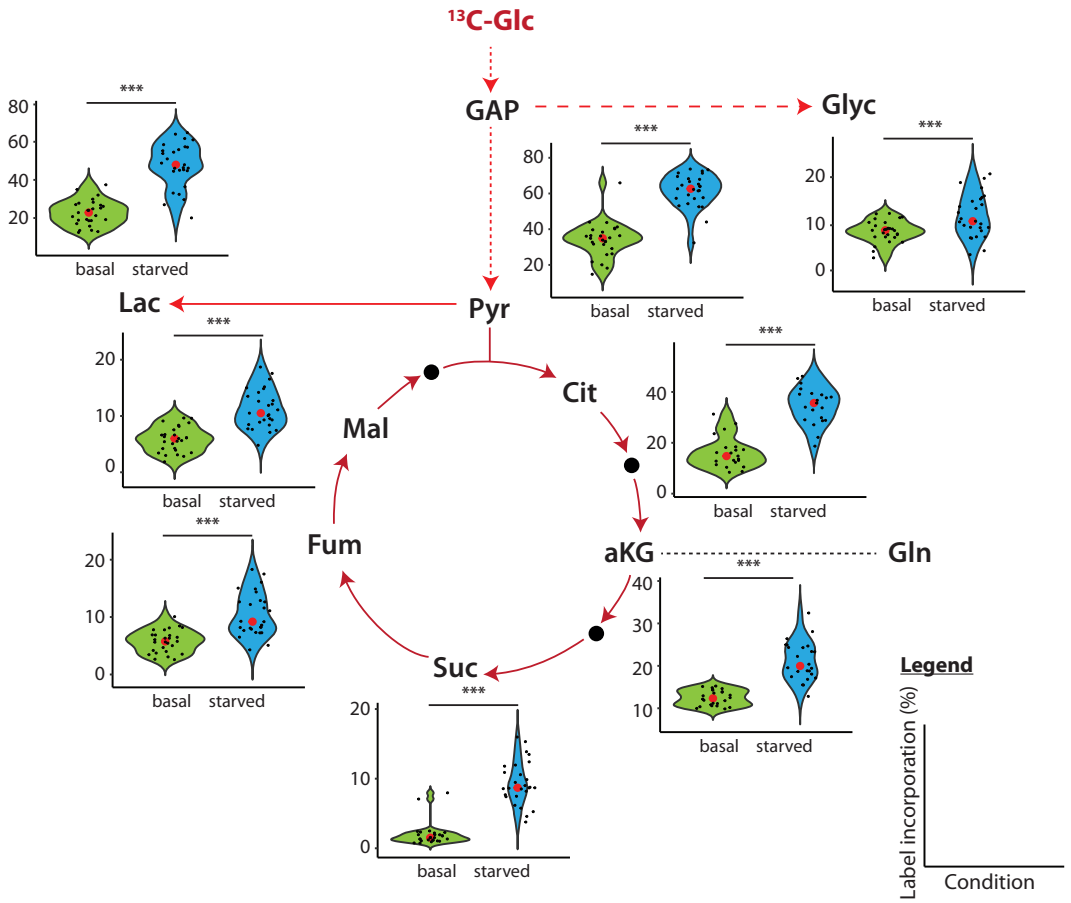


Figure 1. Incorporation of central carbon metabolites after labeling with ^{13}C-glucose for 3 h in both sexes. Violin plots show the individual values, the probability distribution, and the median (red dot) of the label incorporation (in %). Significance was calculated using the paired Wilcoxon rank-sum test. Significance levels are $^{***}P < 0.001$. Depicted are both female and male cells with altogether maximum of 32 data points for 16 twin pairs. The number of biological replicates (pairs for both treatments) for each condition and metabolite is given in Supplemental Table S2*A*. αKG, α-ketoglutaric acid; Cit, citric acid; Fum, fumaric acid; GAP, glyceraldehyd-3-phosphate; Glc, glucose; Gln, glutamine; Glyc, glycerol; Lac, lactic acid; Mal, malic acid; Pyr, pyruvic acid; Suc, succinic acid.

with the rstatix package (version 0.7.2). Data are presented as means ± standard error (SE) unless stated otherwise. For paired comparisons, Wilcoxon signed-rank tests were used to assess statistical significance. Analyses were stratified by growth condition or sex, as indicated. To account for multiple testing, P values were adjusted using the Benjamini–Hochberg false discovery rate (FDR) procedure. Effect sizes were calculated as r, derived from the standardized Wilcoxon test statistic ($r = Z/\sqrt{N}$), where N corresponds to the number of nonzero paired observations. Where possible, 95% confidence intervals for the effect size were calculated. Statistical significance was defined as an unadjusted $P < 0.05$.

RESULTS

A faster label incorporation for both ^{13}C-glucose and ^{13}C-glutamine after serum starvation compared with the basal state in endothelial cells was previously detected by our group, albeit without the consideration of cellular sex (9). We now extended our observations using a higher number of cell donors and analyzed the effects according to sex. For that purpose, we used female and male cells from dizygotic twin pairs. Based on our previous results, we chose 1.5 and 3 h for ^{13}C-glucose and 3 and 6 h for ^{13}C-glutamine labeling to cover the linear range of label incorporation. We selected eight metabolites for incorporation of ^{13}C-glucose (α-ketoglutaric acid, citric acid, fumaric acid, glycerol, lactic acid, malic acid, pyruvic acid, succinic acid) and five metabolites (citric acid in oxidative or reductive state, fumaric acid, malic acid, succinic acid) for ^{13}C-glutamine incorporation.

Regardless of the cellular sex, starvation of endothelial cells led to faster label incorporation for ^{13}C-glucose compared with nonstarved conditions. Already at the early time point of 1.5 h, a highly significant faster label incorporation was detected for all eight metabolites analyzed. A similar result was obtained after 3 h of labeling (Fig. 1, Supplemental Fig. S1).

Labeling with ^{13}C-glutamine led to a similar result as with ^{13}C-glucose. A strong increase in ^{13}C-glutamine label incorporation was detected in serum-starved cells compared with basal conditions. At the early time point of 3 h, a significantly higher label incorporation was observed for all five metabolites after starvation. After 6 h of labeling, incorporation was faster for all five metabolites in serum-starved cells, albeit the difference was not significant for fumaric acid (Fig. 2, Supplemental Fig. S2).

To look for potential sex differences, the results were analyzed for female and male cells separately. Labeling of cells with ^{13}C-glucose under basal conditions resulted in a slightly higher label incorporation for α-ketoglutaric acid, citric acid, pyruvic acid, and succinic acid after 1.5 h in male cells. However, after 3 h of labeling, only citric acid and succinic acid showed a higher label incorporation in male cells (Fig. 3, *A* and *C*). Under serum-starved conditions, citric acid, lactic

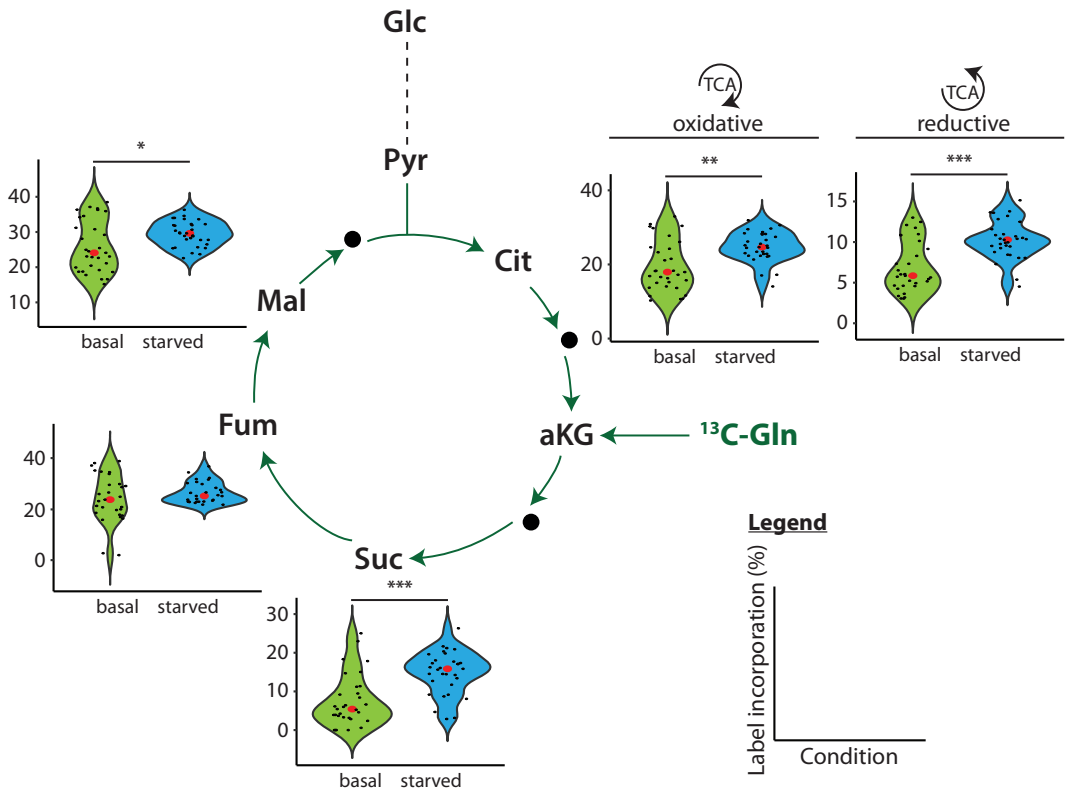


Figure 2. Incorporation of central carbon metabolites after labeling with ^{13}C-glutamine for 6 h in both sexes. Violin plots show the individual values, the probability distribution, and the median (red dot) of the label incorporation (in %). Significance was calculated using the paired Wilcoxon rank-sum test. Significance levels are $*P < 0.05$, $**P < 0.01$, or $***P < 0.001$. Depicted are both female and male cells with altogether max. 32 data points for 16 twin pairs. The number of biological replicates (pairs for both treatments) for each condition and metabolite is given in Supplemental Table S2*B*. αKG, α-ketoglutaric acid; Cit, citric acid; Fum, fumaric acid; Glc, glucose; Gln, glutamine; Mal, malic acid; Pyr, pyruvic acid; Suc, succinic acid; TCA, tricarboxylic acid cycle.

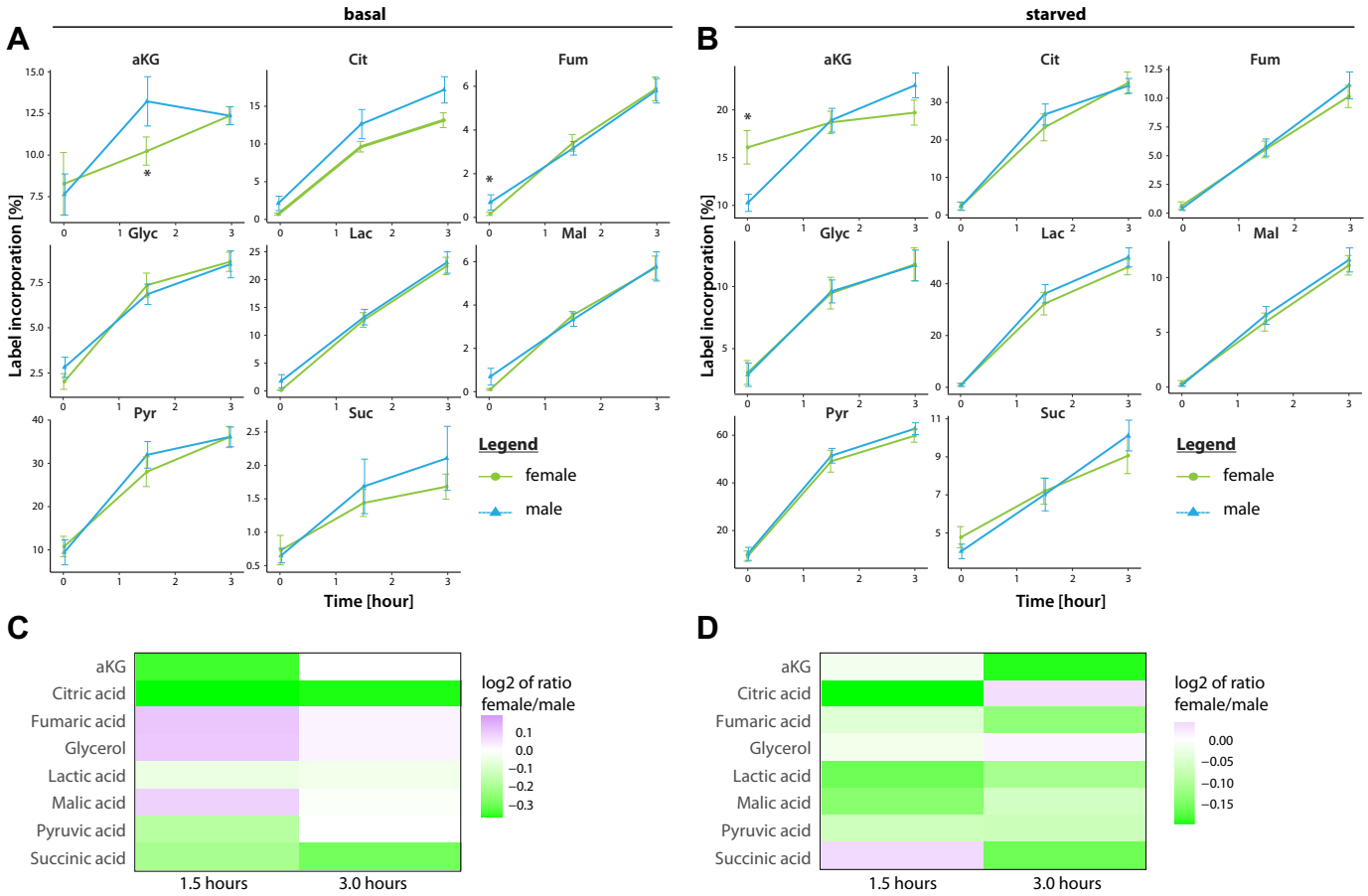


Figure 3. Incorporation of central carbon metabolites after labeling in the presence of ^{13}C-glucose for the indicated time points. Cells were cultured under basal (*A*) or serum-starved (*B*) conditions. The mean and standard error of male and female cells per time point and FCS condition are shown. The heatmap indicates the $\log_2$-transformed ratio of female/male for basal (*C*) and starved (*D*) conditions. Significance between males and females per time point and FCS condition was calculated using the paired Wilcoxon rank-sum test. Significance levels are $^*P < 0.05$. The number of biological replicates (twin pairs) for each condition and metabolite is given in Supplemental Table S3*A*. αKG: α-ketoglutaric acid; Cit, citric acid; Fum, fumaric acid; Glyc, glycerol; Lac, lactic acid; Mal, malic acid; Pyr, pyruvic acid; Suc, succinic acid.

acid, malic acid, and pyruvic acid showed a slightly higher label incorporation in male cells after 1.5 h. After 3 h of labeling, all metabolites, except citric acid and glycerol, exhibited a slightly higher label incorporation in male cells (Fig. 3, *B* and *D*).

Labeling with ^{13}C-glutamine also revealed an apparent sex bias, notable at the later time points. For basal conditions, except for fumaric acid, all metabolites showed a higher label incorporation in female cells after 3 h. After 6 h, all metabolites showed an increased label incorporation in female cells. Interestingly, fumaric acid showed a significant increase in label incorporation in female cells after 6 h (Fig. 4, *A* and *C*). Under serum-starved conditions, label incorporation after the early time point of 3 h was higher only for citric acid (in reductive state) and succinic acid in female cells. After 6 h of labeling, however, all five metabolites revealed a slightly faster label incorporation in female cells compared with male HUVECs (Fig. 4, *B* and *D*).

DISCUSSION

We found small but consistent sex differences in endothelial metabolic flux. Although male cells had a faster metabolic incorporation under serum starvation after ^{13}C-glucose labeling, female cells showed a faster labeling incorporation after ^{13}C-glutamine. These sex differences were observed for almost all detected metabolites after ^{13}C-glucose or ^{13}C-glutamine labeling. Independent of sex, endothelial cells showed an overall faster label incorporation after serum starvation for both labels, strengthening our previous results (9). A faster metabolic label incorporation was also observed in animals after fasting and infection (16, 17). In human whole blood and red blood cells, levels of metabolites increased after fasting. Around one-third of all metabolites had elevated levels after a 58 h fast, including metabolites of the pentose phosphate pathway, purine/pyrimidine metabolites, and the TCA cycle. These metabolic adaptations regulate antioxidant and mitochondrial activity and transcriptional processes like RNA and protein synthesis, finally resulting in a more metabolically active state (18, 19). This finding in humans is supported by our observation of faster label incorporation after serum starvation for a short time at the cellular level. Endothelial cells in vivo play a specialized role in that they have to form new blood vessels under conditions of shortage of oxygen and nutrients (3). To achieve this, they need to remain metabolically active (20). For their energy production, endothelial

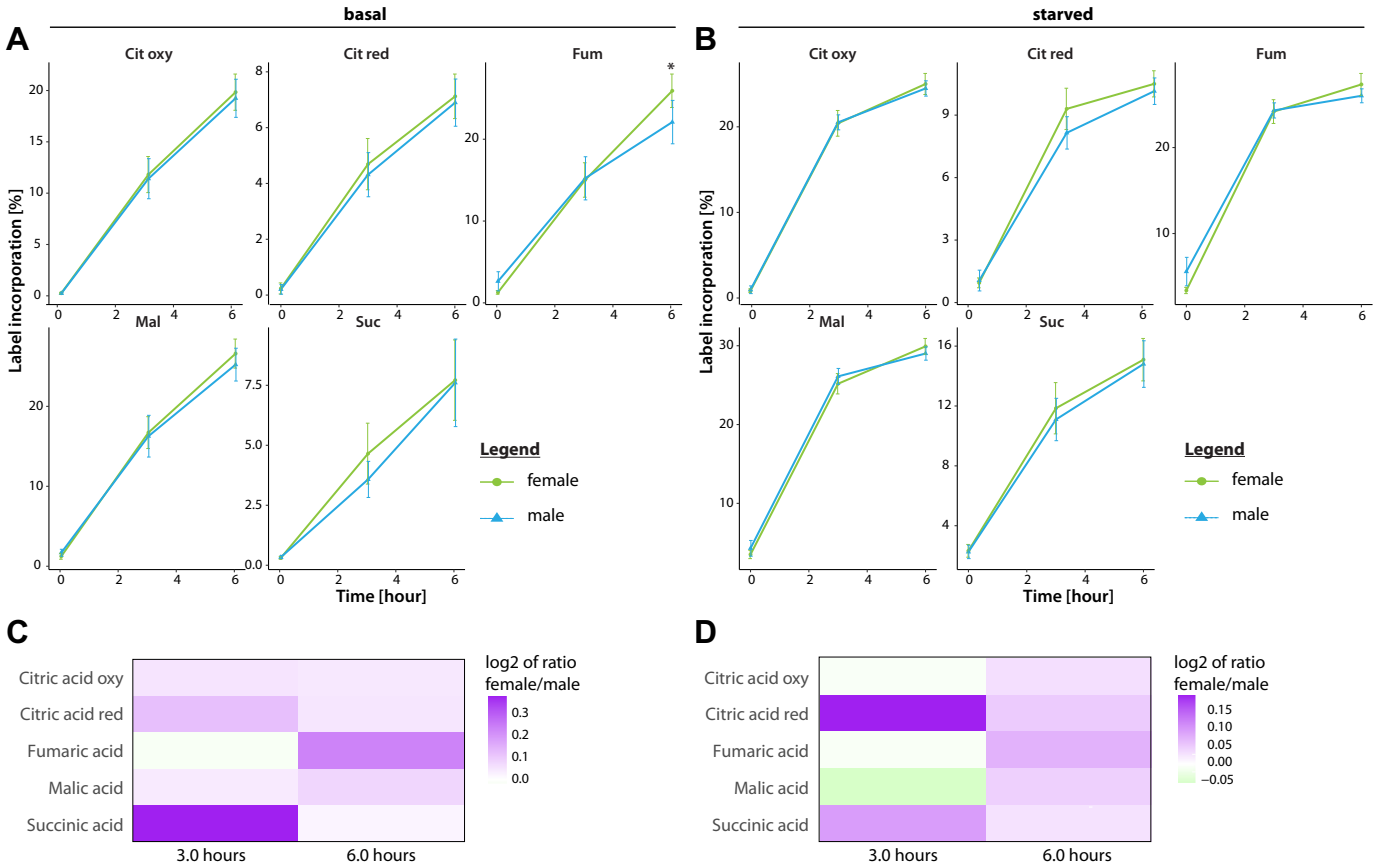


Figure 4. Incorporation of central carbon metabolites after labeling in the presence of ^{13}C-glutamine for the indicated time points. Cells were cultured under basal (*A*) or serum-starved (*B*) conditions. The mean and standard error of male and female cells per time point and FCS condition are shown. The Heatmap indicates the $\log_2$-transformed ratio of female/males for basal (*C*) and starved (*D*) conditions. Significance between males and females per time point and FCS condition was calculated using the paired Wilcoxon rank-sum test. Significance levels are $^*P < 0.05$. The number of biological replicates (twin pairs) for each condition and metabolite is given in Supplemental Table S3*B*. Cit oxy, citric acid in oxidative form; Cit red, citric acid in reductive form; Fum, fumaric acid; Mal, malic acid; Suc, succinic acid.

cells rely on glucose, glutamine, and fatty acids as fuel (2). Cellular proliferation and migration are prerequisites for building new vessels (4). Since these processes require energy, the higher label incorporation after serum starvation would reflect the demand of the cells to increase rather than decrease their metabolic activity. Whether our observation can be generalized to other cell types remains open. In the case of endothelial cells, however, it constitutes the requirement to fulfill their physiological role in the process of angiogenesis at declining nutrient supply.

The rate of label incorporation for female and male cells differed between ^{13}C-glucose and ^{13}C-glutamine in our study at the longer labeling time points. The magnitude of these differences was rather small. In general, sex differences are moderate, but can nevertheless have an important biological impact (21). The observed sex differences in glucose and glutamine metabolism could be, at least in part, mediated by different levels of metabolic enzymes between female and male cells. Although the times of our labeling experiments were rather short (max. 6 h), we reassessed levels of metabolic proteins in our previously published proteomics data (22). However, after serum starvation for 5 h and for 16 h, no major sex differences in levels of enzymes of the glucose and glutamine metabolic pathways were detected in HUVECs from 15 twin pairs (22). This suggests that transcriptional regulation might not be the main driver for the observed sex differences in metabolic flux, but rather potential nongenomic processes could be involved.

Female endothelial cells had a faster incorporation after labeling with ^{13}C-glutamine for all analyzed metabolites, both basal and after serum starvation at the longer time point. In contrast, male cells showed a slightly higher incorporation after ^{13}C-glucose labeling after serum starvation for 6 out of 8 detected metabolites compared with female cells. Endothelial cells are highly glycolytic (23). Under deprivation of nutrients and low oxygen supply, they switch from mitochondrial respiration to aerobic or anaerobic glycolysis (24). During angiogenesis, stalk cells (that form the new vessel) are highly proliferative, and both tip and stalk cells are under a high glycolytic flux to supply enough ATP for cell movement and proliferation (25). Angiogenic treatment of cultured endothelial cells with vascular endothelial growth factor (VEGF) or fibroblast growth factor (FGF) stimulated a high flux of glucose and a high glycolytic rate in these cells (26). The abovementioned findings underline the need for efficient energy production in angiogenic processes and that glucose is mainly used for rapid production of energy. Although the differences are small, the higher label incorporation of glucose in male

cells after serum starvation in our study was consistent for most of the detected metabolites.

In contrast to male cells, we observed a faster incorporation after labeling with ^{13}C-glutamine in female endothelial cells for all analyzed metabolites, both at basal conditions and after serum starvation for 6 h. Glutamine plays a central role in cellular metabolism (27, 28). Although both glucose and glutamine are required as a source of energy, glutamine could be pivotal for endothelial proliferation and migration and especially for maintaining vascular function and viability. Deprivation of glutamine and glutaminase inhibition prevented proliferation of endothelial cells, but not cellular migration. Lack of glutamine catabolism resulted in near complete loss of TCA intermediates, which could not be compensated by glucose-derived anaplerosis (29). Glutamine is used as a nitrogen and carbon source for cellular biomass production to synthesize amino acids, lipids, and nucleic acids. Depletion of glutamine induced apoptosis in endothelial cells. Endothelial-specific deletion of glutaminase or lack of glutamine attenuated vessel sprouting and density in mice and sprouting of endothelial cells due to impaired migration and proliferation, suggesting a pivotal role of glutamine for angiogenesis (29–31). Endothelial deletion of glutamine synthetase reduced vessel sprouting during vascular development in mice (32). Higher levels of glutamine synthetase enhanced reendothelialization of vascular grafts in rats and restored motility, sprouting, and proliferation in cultured endothelial cells (33). In another study, inhibition of glutaminase reduced proliferation, migration, and survival of endothelial cells from different vascular beds, underscoring the role of glutamine metabolism for vascular function (34). In addition to promoting vessel formation and sprouting, glutamine proved to be vital for other cellular processes like membrane integrity, mitochondrial function, and cell viability. Supplementation with glutamine restored hyperglycemia-induced mitochondrial integrity in cultured endothelial cells and reduced oxidative stress and apoptosis (35, 36). Glutamine was also indispensable for the survival of endothelial cells after viral infection (37). In vivo, endothelial cells are under constant flow, which acts as a protective agent against the onset of atherogenic processes. Cultured endothelial cells under shear stress were found to decrease glycolytic metabolism, whereas glutamine anaplerosis was promoted. This illustrates that endothelial cells under favorable flow conditions exhibit a preference for glutamine as a nutrient source and a limited reliance on glycolysis (38).

Summarizing the published observations, glucose is, at least for endothelial cells under static conditions, predominantly utilized as a source for energy production. Whereas glutamine is (beyond energy production) involved in a variety of cellular processes like maintenance of cellular integrity, vascular function, redox status, and cell viability. A faster metabolic incorporation of glutamine in female cells, as found in our study, could therefore provide them with an advantage in maintaining cellular function and viability under unfavorable conditions and deprived nutrient supply. Indeed, in previous studies, we observed a higher migration of female endothelial cells after treatment with VEGF under serum-starved conditions (13). In addition, serum starvation resulted in a higher cellular viability of female cells and a higher rate of apoptosis in male cells (39, 40). Whether these female-based benefits are determined by differences in rates of glucose and glutamine metabolism needs to be proven. But it is tempting to speculate that delicate sex differences in cellular metabolism could lead to sex-specific metabolic adaptations at the cellular level and finally contribute to physiological and pathophysiological sex and gender differences.

In summary, we observed nonsignificant differences in opposite directions between female and male endothelial cells in the rate of metabolic glucose and glutamine incorporation. In light of the essential role of glutamine for overall cellular function, the faster label incorporation of glutamine in female cells could contribute to the described superior capacity of female cells to cope with unfavorable environmental conditions.

DATA AVAILABILITY

Data will be made available from the corresponding author upon reasonable request.

SUPPLEMENTAL MATERIAL

Supplemental Figs. S1 and S2: https://doi.org/10.6084/m9.figshare.33349131.

Supplemental Tables S1–S3: https://doi.org/10.6084/m9.figshare.33349164.

ACKNOWLEDGMENTS

We thank Alina Eisenberger for help with the extraction of the samples. The graphical abstract was initially generated using OpenAI's ChatGPT (GPT-6 Luna) and subsequently extensively edited and refined in Microsoft PowerPoint by the authors.

The tool was used in a manner that does not conflict with APS ethical policies and the authors take full responsibility for the content.

GRANTS

The work was funded by the German Center for Cardiovascular Research, partner site Berlin, Germany (DZHK Berlin, 81Z0100205).

DISCLOSURES

No conflicts of interest, financial or otherwise, are declared by the authors.

AUTHOR CONTRIBUTIONS

M.L. and R.F.-G. conceived and designed research; A.V. and R.F.-G. performed experiments; R.F.-G. analyzed data; M.L., J.W., J.A.K., and R.F.-G. interpreted results of experiments; R.F.-G. prepared figures; M.L. and R.F.-G. drafted manuscript; J.W., A.V., C.B., V.S., K.S., W.H., and J.A.K. edited and revised manuscript; M.L., J.W., A.V., C.B., V.S., K.S., W.H., J.A.K., and R.F.-G. approved final version of manuscript.

REFERENCES

1. **Kersten S.** The impact of fasting on adipose tissue metabolism. *Biochim Biophys Acta Mol Cell Biol Lipids* 1868: 159262, 2023. doi:10.1016/j.bbalip.2022.159262.

2. **Eelen G**, **de Zeeuw P**, **Treps L**, **Harjes U**, **Wong BW**, **Carmeliet P.** Endothelial cell metabolism. *Physiol Rev* 98: 3–58, 2018. doi:10.1152/physrev.00001.2017.
3. **Marziano C**, **Genet G**, **Hirschi KK.** Vascular endothelial cell specification in health and disease. *Angiogenesis* 24: 213–236, 2021. doi:10.1007/s10456-021-09785-7.
4. **Roskoski R Jr.** Vascular endothelial cells and angiogenesis. *Pharmacol Res* 221: 107983, 2025. doi:10.1016/j.phrs.2025.107983.
5. **De Bock K**, **Georgiadou M**, **Carmeliet P.** Role of endothelial cell metabolism in vessel sprouting. *Cell Metab* 18: 634–647, 2013. doi:10.1016/j.cmet.2013.08.001.
6. **Cruys B**, **Wong BW**, **Kuchnio A**, **Verdegem D**, **Cantelmo AR**, **Conradi LC**, **Vandekeere S**, **Bouché A**, **Cornelissen I**, **Vinckier S**, **Merks RM**, **Dejana E**, **Gerhardt H**, **Dewerchin M**, **Bentley K**, **Carmeliet P.** Glycolytic regulation of cell rearrangement in angiogenesis. *Nat Commun* 7: 12240, 2016. doi:10.1038/ncomms12240.
7. **Li X**, **Sun X**, **Carmeliet P.** Hallmarks of endothelial cell metabolism in health and disease. *Cell Metab* 30: 414–433, 2019. doi:10.1016/j.cmet.2019.08.011.
8. **Fraisl P**, **Baes M**, **Carmeliet P.** Hungry for blood vessels: linking metabolism and angiogenesis. *Dev Cell* 14: 313–314, 2008. doi:10.1016/j.devcel.2008.02.009.
9. **Lorenz M**, **Fritsche-Guenther R**, **Bartsch C**, **Vietzke A**, **Eisenberger A**, **Stangl K**, **Stangl V**, **Kirwan JA.** Serum starvation accelerates intracellular metabolism in endothelial cells. *Int J Mol Sci* 24: 1189, 2023. doi:10.3390/ijms24021189.
10. **Costanzo M**, **Caterino M**, **Sotgiu G**, **Ruoppolo M**, **Franconi F**, **Campesi I.** Sex differences in the human metabolome. *Biol Sex Differ* 13: 30, 2022. doi:10.1186/s13293-022-00440-4.
11. **Campesi I**, **Ruoppolo M**, **Franconi F**, **Caterino M**, **Costanzo M.** Sex-gender-based differences in metabolic diseases. *Handb Exp Pharmacol* 282: 241–257, 2023. doi:10.1007/164_2023_683.
12. **Ruoppolo M**, **Scolamiero E**, **Caterino M**, **Mirisola V**, **Franconi F**, **Campesi I.** Female and male human babies have distinct blood metabolomic patterns. *Mol Biosyst* 11: 2483–2492, 2015. doi:10.1039/c5mb00297d.
13. **Lorenz M**, **Blaschke B**, **Benn A**, **Hammer E**, **Witt E**, **Kirwan J**, **Fritsche-Guenther R**, **Gloaguen Y**, **Bartsch C**, **Vietzke A**, **Kramer F**, **Kappert K**, **Brunner P**, **Nguyen HG**, **Dreger H**, **Stangl K**, **Knaus P**, **Stangl V.** Sex-specific metabolic and functional differences in human umbilical vein endothelial cells from twin pairs. *Atherosclerosis* 291: 99–106, 2019. doi:10.1016/j.atherosclerosis.2019.10.007.
14. **Opialla T**, **Kempa S**, **Pietzke M.** Towards a more reliable identification of isomeric metabolites using pattern guided retention validation. *Metabolites* 10: 457, 2020. doi:10.3390/metabo10110457.
15. **Pietzke M**, **Kempa S.** Pulsed stable isotope-resolved metabolomic studies of cancer cells. *Methods Enzymol* 543: 179–198, 2014. doi:10.1016/B978-0-12-801329-8.00009-X.
16. **Butz DE**, **Cook ME**, **Eghbalnia HR**, **Assadi-Porter F**, **Porter WP.** Changes in the natural abundance of 13CO2/12CO2 in breath due to lipopolysacchride-induced acute phase response. *Rapid Commun Mass Spectrom* 23: 3729–3735, 2009. doi:10.1002/rcm.4310.
17. **Doi H**, **Akamatsu F**, **González AL.** Starvation effects on nitrogen and carbon stable isotopes of animals: an insight from meta-analysis of fasting experiments. *R Soc Open Sci* 4: 170633, 2017 [Erratum in *R Soc Open Sci* 4: 171551, 2017]. doi:10.1098/rsos.171551.
18. **Teruya T**, **Chaleckis R**, **Takada J**, **Yanagida M**, **Kondoh H.** Diverse metabolic reactions activated during 58-hr fasting are revealed by non-targeted metabolomic analysis of human blood. *Sci Rep* 9: 854, 2019. doi:10.1038/s41598-018-36674-9.
19. **Kondoh H**, **Teruya T**, **Yanagida M.** Metabolomics of human fasting: new insights about old questions. *Open Biol* 10: 200176, 2020. doi:10.1098/rsob.200176.
20. **Liu Y**, **Wu Z**, **Li Y**, **Chen Y**, **Zhao X**, **Wu M**, **Xia Y.** Metabolic reprogramming and interventions in angiogenesis. *J Adv Res* 70: 323–338, 2025. doi:10.1016/j.jare.2024.05.001.
21. **Stangl V**, **Lorenz M.** Why you should pay more attention to your cells' sex. *J Physiol* 601: 5581–5584, 2023. doi:10.1113/JP284819.
22. **Lorenz M**, **Witt E**, **Völker U**, **Stangl K**, **Stangl V**, **Hammer E.** Serum starvation induces sexual dimorphisms in secreted proteins of human umbilical vein endothelial cells (HUVECs) from twin pairs. *Proteomics* 22: e2100168, 2022. doi:10.1002/pmic.202100168.
23. **Leung SWS**, **Shi Y.** The glycolytic process in endothelial cells and its implications. *Acta Pharmacol Sin* 43: 251–259, 2022. doi:10.1038/s41401-021-00647-y.
24. **De Bock K**, **Georgiadou M**, **Schoors S**, **Kuchnio A**, **Wong BW**, **Cantelmo AR**, **et al.** Role of PFKFB3-driven glycolysis in vessel sprouting. *Cell* 154: 651–663, 2013. doi:10.1016/j.cell.2013.06.037.
25. **Du W**, **Ren L**, **Hamblin MH**, **Fan Y.** Endothelial cell glucose metabolism and angiogenesis. *Biomedicines* 9: 147, 2021. doi:10.3390/biomedicines9020147.
26. **Vizán P**, **Sánchez-Tena S**, **Alcarraz-Vizán G**, **Soler M**, **Messeguer R**, **Pujol MD**, **Lee WN**, **Cascante M.** Characterization of the metabolic changes underlying growth factor angiogenic activation: identification of new potential therapeutic targets. *Carcinogenesis* 30: 946–952, 2009. doi:10.1093/carcin/bgp083.
27. **Wu G**, **Haynes TE**, **Li H**, **Meininger CJ.** Glutamine metabolism in endothelial cells: ornithine synthesis from glutamine via pyrroline-5-carboxylate synthase. *Comp Biochem Physiol A Mol Integr Physiol* 126: 115–123, 2000. doi:10.1016/s1095-6433(00)00196-3.
28. **Yoo HC**, **Yu YC**, **Sung Y**, **Han JM.** Glutamine reliance in cell metabolism. *Exp Mol Med* 52: 1496–1516, 2020. doi:10.1038/s12276-020-00504-8.
29. **Kim B**, **Li J**, **Jang C**, **Arany Z.** Glutamine fuels proliferation but not migration of endothelial cells. *EMBO J* 36: 2321–2333, 2017. doi:10.15252/embj.201796436.
30. **Huang H**, **Vandekeere S**, **Kalucka J**, **Bierhansl L**, **Zecchin A**, **Brüning U**, **Visnagri A**, **Yuldasheva N**, **Goveia J**, **Cruys B**, **Brepoels K**, **Wyns S**, **Rayport S**, **Ghesquière B**, **Vinckier S**, **Schoonjans L**, **Cubbon R**, **Dewerchin M**, **Eelen G**, **Carmeliet P.** Role of glutamine and interlinked asparagine metabolism in vessel formation. *EMBO J* 36: 2334–2352, 2017. doi:10.15252/embj.201695518.
31. **Andrade J**, **Potente M.** New Q(ues) to keep blood vessels growing. *EMBO J* 36: 2315–2317, 2017. doi:10.15252/embj.201797764.
32. **Eelen G**, **Dubois C**, **Cantelmo AR**, **Goveia J**, **Brüning U**, **DeRan M**, **et al.** Role of glutamine synthetase in angiogenesis beyond glutamine synthesis. *Nature* 561: 63–69, 2018. doi:10.1038/s41586-018-0466-7.
33. **Wei X**, **Wang L**, **Xing Z**, **Chen P**, **He X**, **Tuo X**, **Su H**, **Zhou G**, **Liu H**, **Fan Y.** Glutamine synthetase accelerates re-endothelialization of vascular grafts by mitigating endothelial cell dysfunction in a rat model. *Biomaterials* 314: 122877, 2025. doi:10.1016/j.biomaterials.2024.122877.
34. **Peyton KJ**, **Liu XM**, **Yu Y**, **Yates B**, **Behnammanesh G**, **Durante W.** Glutaminase-1 stimulates the proliferation, migration, and survival of human endothelial cells. *Biochem Pharmacol* 156: 204–214, 2018. doi:10.1016/j.bcp.2018.08.032.
35. **Safi SZ**, **Batumalaie K**, **Mansor M**, **Chinna K**, **Mohan S**, **Karimian H**, **Qvist R**, **Ashraf MA**, **Yan GO.** Glutamine treatment attenuates hyperglycemia-induced mitochondrial stress and apoptosis in umbilical vein endothelial cells. *Clinics (Sao Paulo)* 70: 569–576, 2015 [Erratum *in Clinics (Sao Paulo)* 70: 827, 2015]. doi:10.6061/clinics/2015(08)07.
36. **Yu M**, **Chen H**, **Chen C**, **Zhao C**, **Zhou Q**, **Xie L**, **Wang T.** Hyperglycemia-depleted glutamine contributes to the pathogenesis of diabetic corneal endothelial dysfunction. *Exp Eye Res* 249: 110124, 2024. doi:10.1016/j.exer.2024.110124.
37. **Sanchez EL**, **Carroll PA**, **Thalhofer AB**, **Lagunoff M.** Latent KSHV infected endothelial cells are glutamine addicted and require glutaminolysis for survival. *PLoS Pathog* 11: e1005052, 2015. doi:10.1371/journal.ppat.1005052.
38. **Simões-Faria R**, **Daems M**, **Peacock HM**, **Declercq M**, **Willems A**, **Jones EAV**, **Ghesquière B.** Wall shear stress modulates metabolic pathways in endothelial cells. *Metabolomics* 21: 16, 2025. doi:10.1007/s11306-024-02214-y.
39. **Lorenz M**, **Koschate J**, **Kaufmann K**, **Kreye C**, **Mertens M**, **Kuebler WM**, **Baumann G**, **Gossing G**, **Marki A**, **Zakrzewicz A**, **Miéville C**, **Benn A**, **Horbelt D**, **Wratil PR**, **Stangl K**, **Stangl V.** Does cellular sex matter? Dimorphic transcriptional differences between female and male endothelial cells. *Atherosclerosis* 240: 61–72, 2015. doi:10.1016/j.atherosclerosis.2015.02.018.
40. **Cattaneo MG**, **Banfi C**, **Brioschi M**, **Lattuada D**, **Vicentini LM.** Sex-dependent differences in the secretome of human endothelial cells. *Biol Sex Differ* 12: 7, 2021. doi:10.1186/s13293-020-00350-3.